euspen's 19th International Conference & Exhibition, Bilbao, ES, June 2019
www.euspen.eu

The influence of flexibility on the force balance quality: a frequency domain approach

J.J. de Jong[1], B.E.M. Schaars[1], D.M. Brouwer[1]

[1]*University of Twente, Enschede, The Netherlands, Precision Engineering Lab*

j.j.dejong@utwente.nl

Abstract
High accelerations of fast moving robots induce high fluctuating reaction forces and moments, resulting in undesirable vibrations and loss of accuracy. These fluctuations can be reduced or even eliminated by dynamic balancing techniques, e.g. by addition of counter-masses. However, these techniques typically disregard the flexibility of the mechanism. This flexibility potentially leads to undesirable eigenfrequencies and unbalance of an otherwise perfectly balanced mechanism. In this paper, the effect of link flexibility on the force balance quality is investigated in the frequency domain. This is done for a 2-DOF parallel manipulator with realistic stiffnesses. With the use of flexible multi-body software, the frequency transfer functions for the shaking forces are obtained for an unbalanced, a force balanced and a partially balanced case. The results show that, firstly, force balance results in a strong attenuation of the shaking forces' frequency content up to the first eigenfrequency. Secondly, the addition of balance mass results in a reduction of the first parasitic eigenfrequency of the system leading to a worsened performance around the first eigenfrequency and a reduction in controller bandwidth. Identification of these effects leads to an optimal, intermediate solution, which mitigates the negative effects of dynamic balance, resulting in low-frequency shaking force attenuation of 30 dB without loss of controller bandwidth.

Keywords: dynamic balance, vibration isolation, parallel manipulators.

1. Introduction

Dynamic balance aims to eliminate changing reaction forces and moments of high-speed robots by design of the mass distribution [1], [2]. Essentially, this leads to a dynamic decoupling between the robot and surroundings, reducing the vibration propagation and potentially eliminating the need for vibration isolation measures such as force frames, heavy soft mounts, and active vibration isolation [3].

Typically, an addition of counter-masses is required for dynamic balance, leading to increased mass, motor torques and bearing forces. These effects can be mitigated by choice of an intermediate, partial balancing solution [4]–[6]. Moreover, the added mass is expected to lower the eigenfrequecies of the mechanisms leading to increased vibrations, and lower controller bandwidth. This is confirmed by [7]–[10], which have reported significant shaking forces, when considering link flexibility of an otherwise force balanced linkage. The literature on dynamic balancing of flexible linkages has focused on the time analysis of single degree of freedom (DOF), fixed speed, input-output machines. To the our best knowledge, only Martini et al. [11], [12] have performed a modal analysis on both unbalanced and dynamically balanced mechanisms. Still, the exact consequence of these lowered eigenfrequencies on the frequency response of multi-DOF manipulators has not been shown. Moreover, it remains unclear under which conditions dynamic balancing of robots with realistic stiffnesses is beneficial at all.

In this paper, a frequency domain method for quantifying the dynamic balance quality of finitely stiff mechanisms is presented and applied to a 2-DOF planar mechanism leading to a novel dynamic balance design criterion. In the following sections, the mechanism design, its balancing solutions, and the evaluation method of the balancing performance are presented. Additionally, the resulting transfer functions are shown and qualitatively compared to a parametric model, leading to optimal design criterions for the dynamic balance of flexible robots.

2. Methods

The influence of flexibility on the force balancing quality is assessed for three cases: 1) unbalanced, 2) fully force balanced and 3) partially balanced.

2.1. Unbalanced mechanism

The robotic system under evaluation is shown in Fig. 1. The dimensions (Table 1) are chosen to resemble a commercially

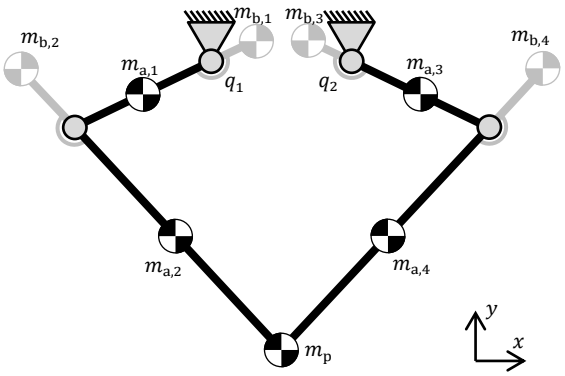

Figure 1. The 2-DOF planar mechanism with counter-masses in grey

Table 1. Robot design parameters

Name	Symbol	Value	Unit
Base width	l_s	160	mm
Upper arm length	$l_{\mathrm{a},1}, l_{\mathrm{a},3}$	260	mm
Upper arm outer diameter		60	mm
Upper arm inner diameter		40	mm
Upper arm mass	$m_{\mathrm{a},1}, m_{\mathrm{a},3}$	3.19	kg
Lower arm length	$l_{\mathrm{a},2}, l_{\mathrm{a},4}$	510	mm
Lower arm outer diameter		30	mm
Lower arm inner diameter		20	mm
Lower arm mass	$m_{\mathrm{a},2}, m_{\mathrm{a},4}$	0.34	kg
Payload	m_p	1	kg

available robot [13] with a workspace of approximately 800 mm × 250 mm. The upper and lower arms ($l_{\mathrm{a},i}$) have a respective length of 260 mm and 510 mm. The payload (m_p) on the end-effector is 1 kg. For evaluating the flexibility of system, the upper arms are modelled as steel tubes with an outer and inner diameter of 60 mm and 40 mm, respectively. The lower arms are carbon tubes with an outer and inner diameter of 30 mm, and 20 mm, respectively. The links of the robot are modeled as fully elastic beams.

2.2. Force balanced mechanism

A mechanism is force balanced when the total center of mass is stationary for all admissible motion. According to [14], this places 6 conditions on the link counter-mass ($m_{\mathrm{b},i}$) and counter-mass location ($l_{\mathrm{b},i}$). A symmetric force balance solution with in-line counter-masses is chosen, such that the following design equations hold

$$m_{\mathrm{b},2} l_{\mathrm{b},2} = \frac{1}{2}\left(m_{\mathrm{a},2} + m_\mathrm{p}\right) l_{\mathrm{a},2} \tag{1}$$

$$m_{\mathrm{b},1} l_{\mathrm{b},1} = \left(m_{\mathrm{a},2} + m_{\mathrm{b},2} + \frac{1}{2} m_\mathrm{p}\right) l_{\mathrm{a},1} \tag{2}$$

$$m_{\mathrm{b},1} l_{\mathrm{b},1} = m_{\mathrm{b},3} l_{\mathrm{b},3}\,, \qquad m_{\mathrm{b},1} = m_{\mathrm{b},3} \tag{3,4}$$

$$m_{\mathrm{b},2} l_{\mathrm{b},2} = m_{\mathrm{b},4} l_{\mathrm{b},4}, \qquad m_{\mathrm{b},2} = m_{\mathrm{b},4} \tag{5,6}$$

From these equations either the counter-mass ($m_{\mathrm{b},i}$) or the counter-mass location can be chosen ($l_{\mathrm{b},i}$). A solution with minimal lengths of the counter-mass links is a common choice in literature [15]. Although this will result in large counter-masses, the moments of inertia and hence the motor torques are then minimal. The counter-masses on the lower arms are to be balanced by the counter-masses on the upper arm, leading to a significant increase of the total mass. Based on practical considerations, the counter-mass location is chosen to be 39 mm and 51 mm for the upper and lower arm respectively (Table 2). This results in counter-masses of 60.8 kg for the upper arms and 6.7 kg for the lower arms.

2.3. Partially balanced mechanism

The large addition of mass can be mitigated by adopting a partial dynamic balance solution [16]. The optimal design parameters are strongly dependent on the trajectory selection,

Table 2. Counter-mass properties for the force balanced (FB) and partially balanced (PB) case.

Name	Symbol	FB	PB	Unit
Upper arm counter-mass	$m_{\mathrm{b},1}, m_{\mathrm{b},3}$	60.8	17.0	kg
Upper arm counter-mass location	$l_{\mathrm{b},1}, l_{\mathrm{b},3}$	39	39	mm
Lower arm counter-mass	$m_{\mathrm{b},2}, m_{\mathrm{b},4}$	6.7	-	kg
Lower arm counter-mass location	$l_{\mathrm{b},2}, l_{\mathrm{b},4}$	51	-	mm

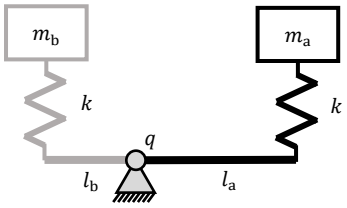

Figure 2. The parametric model of the dynamically balanced mechanism. The counter-mass is depicted in grey.

and the desired trade-off between actuator torques, shaking moments and shaking forces. Here, for the partial balancing solution, only counter-masses on the two upper links are used. The location of the counter-masses are identical to the fully force balanced mechanism. The counter-masses are chosen such that the shaking forces are minimal for a horizontal trajectory through the middle of the workspace. This resulted in counter-masses of 17 kg (Table 2).

2.4. Evaluation of the force balance quality

Evaluation of the shaking force balance quality for these three cases is performed by comparing the transfer functions $T(s)$ from one actuator angle (q) to the shaking forces (f) at the base.

$$T(s) = \frac{f(s)}{q(s)} \tag{7}$$

In this transfer function, s denotes the complex frequency. These transfer functions are obtained by modeling and linearization of the mechanism in a numerical flexible multi-body software package [17].

In order to obtain this transfer function, the linearization requires the assumption that the joint angle can be perfectly controlled. This assumption implies that the joint angle is virtually fixed. Such a perfect controller does not exist; in fact, the performance of the controller is limited by the first parasitic eigenfrequency. Close to this first parasitic eigenfrequency, the controller has no effect and joint behaves as a released or 'free' joint. This model choice - for fixture or release - influences the modeshape and therefore the eigenfrequencies of system. To clearly make the distinction between these two cases also two linearizations are made, one in which the joint angle is fixed in order to obtain the joint to shaking force transfer function, and a second with the input joints released to obtain the first parasitic eigenfrequency and mode which are limiting the bandwidth of the controller.

2.5. Parametric model

The observed behavior in numerical simulation is explained by comparing it to a simplified analytic parametric model of a single balanced elastic beam. This beam is modeled as two spring-mass-systems hinged at the base (Fig. 2). The right mass-spring system represents the unbalanced mechanism and the left system the counter-mass system. The frequency transfer functions of the left (P_a) and right (P_b) mass-spring system from joint rotation to shaking force in the vertical direction become:

$$P_{\mathrm{UB}}(s) = P_\mathrm{a} = \frac{m_\mathrm{a} l_\mathrm{a} k s^2}{m_\mathrm{a} s^2 + k}, \qquad P_\mathrm{b} = \frac{m_\mathrm{b} l_\mathrm{b} k s^2}{m_\mathrm{b} s^2 + k} \tag{8,9}$$

In which m_a, m_b, l_a, and l_b are the masses and lengths of both systems. For convenience the same stiffness (k) for both systems is chosen. With force balance and partial balance the two mass-spring systems are combined, leading to the following total transfer function:

$$P_{\mathrm{PB}} = P_\mathrm{a} - P_\mathrm{b} = \frac{(m_\mathrm{a} l_\mathrm{a} - m_\mathrm{b} l_\mathrm{b}) k^2 s^2 + m_\mathrm{a} m_\mathrm{b} (l_\mathrm{a} - l_\mathrm{b}) k s^4}{(m_\mathrm{a} s^2 + k)(m_\mathrm{b} s^2 + k)} \tag{10}$$

The force balance condition of this beam is:

$$0 = m_\mathrm{a} l_\mathrm{a} - m_\mathrm{b} l_\mathrm{b} \tag{11}$$

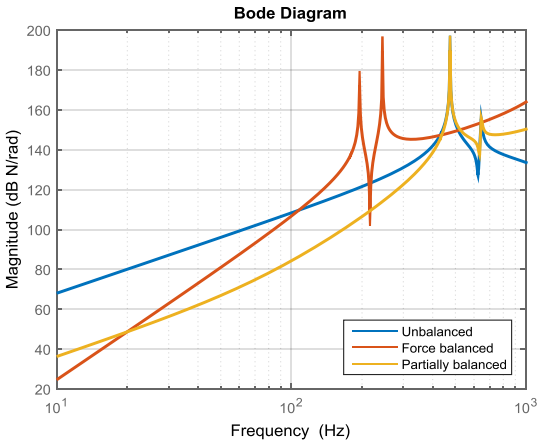

Figure 3. The shaking force frequency content of the 2-DOF mechanism in the vertical direction due to actuation of joint 1. The units of the y-axis are the logarithm of N/rad.

Therefore, the transfer function of the force balance system becomes

$$P_{\mathrm{FB}} = \frac{m_{\mathrm{a}} m_{\mathrm{b}} (l_{\mathrm{a}} - l_{\mathrm{b}}) k s^4}{(m_{\mathrm{a}} s^2 + k)(m_{\mathrm{b}} s^2 + k)} \tag{12}$$

Here it can be seen that force balance eliminates the s^2 component in the numerator of (10).

3. Results

The linearization of the full dynamic model of the 2-DOF mechanism around the midpoint of the workspace results in a frequency transfer function (Fig. 3.) from joint angle 1 in rad to shaking forces in the y-direction in Nm. The modes shapes of the fixed-joint linearization are depicted in Fig. 4. The modes shapes of the released-joint linearization are shown in Fig. 5. Table 3 provides the eigenfrequencies of both linearizations.

3.1. Unbalanced mechanism

A low frequent 40 dB/decade line characterizes the transfer function of the shaking forces of the unbalanced mechanisms until the fixed-joint eigenfrequency at 474 Hz (Fig. 3). Beyond this eigenfrequency, the internal vibrations of the robot are dominant. Since the shaking forces of a rigid body motion correspond to $f_y = m_{\mathrm{eq}} \ddot{q}_1$, the Laplace domain the transfer function is characterized by $T_{\mathrm{UB}} \approx m_{\mathrm{eq}} s^2$. In here m_{eq} is the equivalent mass inducing the shaking force. This s^2 result in 40 dB/decade line and is termed the rigid body motion effects of the robot.

This effect is also observed in the parametric model. In the frequency region far below the first eigenfrequency ($\omega \ll \omega_1$) the behavior of the unbalanced mechanism (8) can be approximated by

$$P_{\mathrm{UB}} \approx m_{\mathrm{a}} l_{\mathrm{a}} s^2 \tag{12}$$

It can be seen that here the rigid body behavior is dominant. This corresponds to a 40 dB/decade line in the bode diagram.

Inspection of the fixed-joint eigenmodes of the mechanism (Fig. 4a and d) reveals that the first eigenmode (433 Hz) is in the x-direction, and does not contribute in the y-direction transfer function. This is attributed to the symmetry of the robot in this pose.

The controller bandwidth is limited by the released-joint first parasitic eigenfrequency (Fig. 5a). This is 620 Hz in the unbalanced case.

3.2. Force balanced mechanism

The transfer function of the fully force balanced mechanism is characterized by an 80 dB/decade line up to the first fixed-joint eigenfrequency. This shows that force balance removes the rigid body effect on the force vibrations such that the transfer function in this domain is characterized by $T(s) \approx m_{\mathrm{eq}} s^4$. From the parametric model, a similar low-frequent approximation is found:

$$P_{\mathrm{FB}} \approx \frac{m_{\mathrm{a}} m_{\mathrm{b}} (l_{\mathrm{a}} - l_{\mathrm{b}})}{k} s^4 \tag{14}$$

This fourth-order behavior corresponds to the 80 dB/decade line of the numeric simulation. This shows that dynamic balance results in a strong attenuation of the shaking forces in the frequency region below the first eigenfrequency.

Additionally, the first fixed-joint eigenfrequency of the system is lowered from 433 Hz to 179 Hz due to counter-masses placed at the lower arms. Therefore, the force balance quality of this flexible manipulator is improved in the low frequency range up to 108 Hz; beyond this frequency, the performance is worsened.

The lowering of the eigenfrequencies due to dynamic balance is also observed in the released-joint eigenfrequency; the first parasitic eigenfrequency is lowered to 204 Hz, indicating a significant loss of controller bandwidth.

3.3. Partially balanced mechanism

The partially balanced robot shares a low frequent 40 dB/decade line with the unbalanced mechanism. However, the magnitude of this line is lower compared to the unbalanced case. Effectively, this results in a 30 dB reduction in low-frequent region. This is attributed to the reduction of the equivalent mass.

In the parametric model, the shaking forces at the frequencies below the first eigenfrequency are dominated by

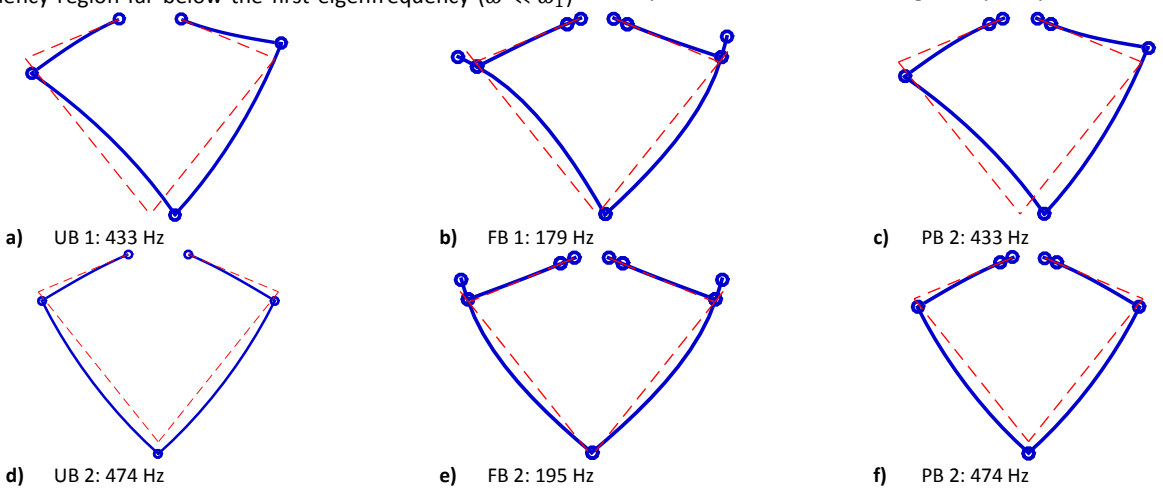

Figure 4. The first two fixed-joint mode shapes for the unbalanced (a, d), force balanced (b, e) and partially balanced case (c,f)

Table 3. The first unwanted eigenfrequencies (in Hz) for the fixed-joint ($\omega_{\mathrm{f},i}$) and released-joint ($\omega_{\mathrm{r},i}$) linearizations in the unbalanced (UB), force balanced (FB) and partially balanced case (PB).

Case	$\omega_{\mathrm{f},1}$	$\omega_{\mathrm{f},2}$	$\omega_{\mathrm{r},1}$	$\omega_{\mathrm{r},2}$
Unbalanced	433	474	620	624
Force balanced	179	195	204	213
Partially balanced	433	474	619	621

the rigid body effects as seen from the following approximation

$$P_{\mathrm{PB}} \approx (m_{\mathrm{a}} l_{\mathrm{a}} - m_{\mathrm{b}} l_{\mathrm{b}}) s^2 \tag{15}$$

In here also the rigid-body, second-order behavior is found. The difference between the unbalanced case is a reduction of the effective mass by suitable choice of the counter-mass ($m_{\mathrm{b}} l_b$).

Additionally, a minimal decrease of the first released-joint parasitic eigenfrequencies to 619 Hz occurs. Since the counter-masses are placed at the base joints, solely the higher, non-critical eigenfrequencies are reduced. This indicates that the controller bandwidth can be maintained with partial dynamic balance.

4. Conclusion

In this paper, it is shown that dynamic balance results in a low frequent attenuation of the shaking forces of 40 dB/decade in comparison to an unbalanced robot. This effect is due to the elimination of the rigid body contribution in the shaking force. This is particularly helpful if a shaking force attenuation is required in the low frequency range. However, the added balance mass also lowers the first parasitic eigenfrequency. In the present case study a reduction of 67 %, from 620 Hz to 204 Hz was observed. This will result in a proportional loss of controller bandwidth and hence performance the robot. Partial dynamic balance combines a low frequent attenuation without a reduction of the first parasitic eigenfrequency and is therefore suited to maintain the controllability of the robot. The proposed frequency domain analysis of the dynamic balance quality enables a dynamic balance solutions tailored to application specific needs.

References

[1] V. H. Arakelian and M. R. Smith, "Shaking Force and Shaking Moment Balancing of Mechanisms: A Historical Review With New Examples," *J. Mech. Des.*, vol. 127, no. 2, p. 334, 2005.

[2] V. H. Arakelian and M. R. Smith, "Erratum: 'Shaking Force and Shaking Moment Balancing of Mechanisms: A Historical Review With New Examples,'" *J. Mech. Des.*, vol. 138, no. December 2016, p. 128001, 2005.

[3] V. Van der Wijk, "Methodology for analysis and synthesis of inherently force and moment-balanced mechanisms - theory and applications," 2014.

[4] J.-F. Collard and C. M. Gosselin, "Optimal Synthesis of a Planar Reactionless Three-Degree-of-Freedom Parallel Mechanism," *J. Mech. Robot.*, vol. 3, no. 4, p. 041009, 2011.

[5] I. S. Kochev, "General theory of complete shaking moment balancing of planar linkages: a critical review," *Mech. Mach. Theory*, vol. 35, no. 11, pp. 1501–1514, Nov. 2000.

[6] M. Verschuure, B. Demeulenaere, J. Swevers, and J. De Schutter, "Counterweight Balancing for Vibration Reduction of Elastically Mounted Machine Frames: A Second-Order Cone Programming Approach," *J. Mech. Des.*, vol. 130, no. 2, p. 022302, 2008.

[7] M. J. Walker and R. S. Haines, "An experimental study of the effects of counterweights on a six-bar chain," *Mech. Mach. Theory*, vol. 17, no. 6, pp. 355–360, 1982.

[8] E. Raghu and A. Balasubramonian, "Experimental study on the elastodynamic behavior of the unbalanced and the counterweighted four bar mechanisms," *J. Mech. Des.*, vol. 112, no. 3, pp. 271–277, 1990.

[9] X. Fengfeng and R. Sinatra, "Effect of dynamic balancing on four-bar linkage vibrations," *Mech. Mach. Theory*, vol. 32, no. 6, pp. 715–728, 1997.

[10] M. A. K. Zobairi, S. S. Rao, and B. Sahay, "Kineto-elastodynamic balancing of 4R-four bar mechanisms combining kinematic and dynamic stress considerations," *Mech. Mach. Theory*, vol. 21, no. 4, pp. 307–315, 1986.

[11] A. Martini, M. Troncossi, M. Carricato, and A. Rivola, "Elastodynamic behavior of balanced closed-loop mechanisms : numerical analysis of a four-bar linkage," pp. 601–614, 2014.

[12] A. Martini, M. Troncossi, M. Carricato, and A. Rivola, "Modal and Kineto-elastodynamic Analyses of Balanced Four-bar Linkages," *ECCOMAS, Multibody Dyn. 2009, 29 June-2 July 2009, Warsaw, Pol.*, no. July, pp. 1–20, 2009.

[13] Codian Robotics, "Robots, Twee-dimensionale delta." [Online]. Available: https://www.codian-robotics.com/d2-robots. [Accessed: 13-Dec-2018].

[14] P. R. Ouyang, Q. Li, and W. J. Zhang, "Integrated design of robotic mechanisms for force balancing and trajectory tracking," *Mechatronics*, vol. 13, no. 8–9, pp. 887–905, Oct. 2003.

[15] V. Van der Wijk and J. L. Herder, "Dynamic Balancing of Clavel's Delta Robot," in *Computational Kinematics*, 2009, pp. 315–322.

[16] J. J. De Jong, J. P. Meijaard, and V. Van der Wijk, "The influence of partial force balancing on the shaking moments, contact forces, and precision of a delta robot-Like manipulator in a compliant frame," in *Proceedings 2018 ASME IDETC/CIE*, 2018, pp. 1–7.

[17] J. B. Jonker, R. G. K. M. Aarts, and J. Van Dijk, "A linearized input-output representation of flexible multibody systems for control synthesis," *Multibody Syst. Dyn.*, vol. 21, no. 2, pp. 99–122, 2009.

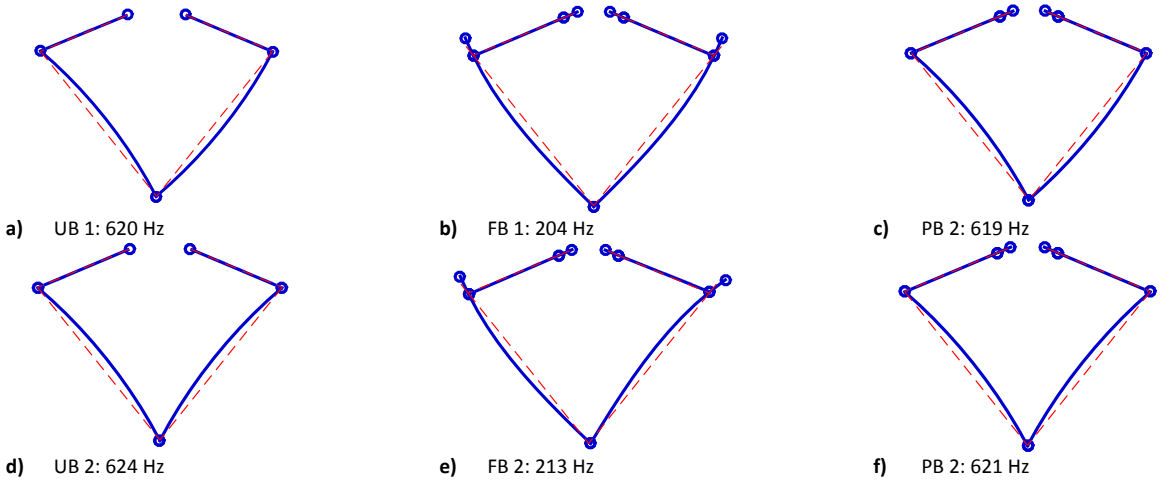

a) UB 1: 620 Hz **b)** FB 1: 204 Hz **c)** PB 2: 619 Hz

d) UB 2: 624 Hz **e)** FB 2: 213 Hz **f)** PB 2: 621 Hz

Figure 5. The first two released-joint mode shapes for the unbalanced (a, d), force balanced (b, e) and partially balanced case (c,f)